第 24 卷第 2 期 无 机 化 学 学 报 Vol.24 No.2
2008 年 2 月 CHINESE JOURNAL OF INORGANIC CHEMISTRY 218~224

Ba_2InSbO_6 双钙钛矿的水热合成及 ^{121}Sb Mössbauer 谱表征

梅晓岩[2] 别利剑[3] 马程浩[1] 黄洪波[4] 刘荣厚[2] 郑文君*,[1] 夏元复[4]
([1] 南开大学化学学院材料化学系,天津 300071)
([2] 上海交通大学农业与生物学院,上海 200240)
([3] 天津理工大学材料科学与工程学院,天津 300191)
([4] 南京大学物理系,南京 210093)

摘要: 在温和水热条件下,合成了双钙钛矿型 Ba_2InSbO_6,采用 XRD、TEM、XPS、ICP 及 IR 等技术表征产物的结构及组成。XRD 数据的 Rietveld 拟合结果表明,Ba_2InSbO_6 为 a=0.416 782(13) nm 的立方钙钛矿结构,属于 $Pm\bar{3}m$。^{121}Sb Mössbauer 谱测试表明,产物的同质异能移可归属为 Sb^V 及 Sb-O 键具有明显的共价特征。合成条件的研究表明,Sb 源对合成具有重要影响,且 Sb_2O_3 锑源可有效地降低杂质的生成。

关键词: 水热合成; ^{121}Sb Mössbauer 谱; 双钙钛矿型氧化物; Ba_2InSbO_6
中图分类号: O611.2; O614.23+3; O614.53+1 **文献标识码**: A **文章编号**: 1001-4861(2008)02-0218-07

Hydrothermal Synthesis and ^{121}Sb Mössbauer Characterization of Double Perovskite Ba_2InSbO_6

MEI Xiao-Yan[2] BIE Li-Jian[3] MA Cheng-Hao[1] HUANG Hong-Bo[4]
LIU Rong-Hou[2] ZHENG Wen-Jun[1]* XIA Yuan-Fu[4]
([1] *Department of Materials Chemistry, College of Chemistry, Nankai University, Tianjin* 300071)
([2] *School of Agriculture and Biology, Shanghai JiaoTong University, Shanghai* 200240)
([3] *College of Materials Science & Engineering, Tianjin University of Technology, Tianjin* 300191)
([4] *Department of Physics, Nanjing University, Nanjing* 210093)

Abstract: A double perovskite-type Ba_2InSbO_6 was prepared by a mild hydrothermal process. The product was characterized by XRD, TEM, XPS, ICP and IR techniques. Primary structural determination using Rietveld method based on XRD data shows that Ba_2InSbO_6 is indexed with a cubic cell and assigned to space group $Pm\bar{3}m$ with a= 0.416 782(13) nm. Measurement of the Mössbauer effect of the 37.2 keV γ transition of ^{121}Sb indicats that the isomer shift falls in the region of the Sb^V and reflects some hybridized-orbital behavior. The influences of hydrothermal conditions on the synthesis were investigated. Then Sb source plays an important role and impurities are significantly decreased when Sb_2O_3 is used as the Sb source.

Key words: hydrothermal synthesis; ^{121}Sb Mössbauer; double perovskite oxide; Ba_2InSbO_6

Perovskite-type oxides have attracted considerable attention because of their technological applications and academic interest. Among A_2SbMO_6 perovskite-type oxides, the ones with compositions containing A-cations (A=Ca, Sr, Ba) and B-cations (M=Sc, Cr, Mn, Fe, Co, Ni, Ru, Bi, In, Ga, Bi, Y, Nd, Gd and Rh) have already

收稿日期:2007-08-30。收修改稿日期:2007-11-06。
国家自然科学基金(No.20273033,20571044)、南开大学本科生科研百项创新工程资助项目。
*通讯联系人。E-mail:zhwj@nankai.edu.cn
第一作者:梅晓岩,男,39 岁,教授;研究方向:无机材料化学、生物质能源。

been reported[1]. The $A_2BB'O_6$-type perovskites with an ordered distribution of B-cations are most probable when large differences exist in either charges or ionic radii[2], while the B-cations ordering degree generally depends on synthesis or annealing temperatures[3]. Moreover, A_2MSbO_6 (A=Ba, Sr and M=Sc, In and Ga) can be used as the substrates and buffer layers for high-Tc superconducting $YBa_2Cu_3O_7$[1f,1g].

Hydrothermal routes to oxides synthesis have attracted a great deal of interest[4]. So far, most literatures on hydrothermal synthesis of perovskite-type oxides with B-cation of two and more have focused mainly on minor dopants[5] or similar charges and radii of B-cations[6]. Only a few papers demonstrate the synthesis of ordered double perovskite-type oxides[7] to the best of our knowledge. For the synthesis of double perovskite-type oxides, the size difference and variety of the B-cations are not only responsible for the applied range of hydrothermal process, but also play a very important role to control the B-cations ordering degree. For these reasons, we focused our attention on the hydrothermal synthesis of double perovskite-type oxides.

The aim of the present paper is to determine the crystal structure, and to evaluate the valence state of the Sb in Ba_2InSbO_6 synthesized by the hydrothermal method. ^{121}Sb Mössbauer spectroscopy was used to investigate the valence state of Sb in connection with powder X-ray diffraction (XRD) and X-ray photo electron spectroscopy (XPS) measurements.

1 Experimental

1.1 Synthesis

$Ba(OH)_2 \cdot 8H_2O$, In_2O_3, Sb_2O_5 or Sb_2O_3, H_2O_2, and KOH were used as the starting materials. The typical synthesis is as follows: First, a 0.2 mol·L^{-1} $Ba(OH)_2$ solution was prepared in de-ionized water; the other reactants were added to the solution in sequence of In_2O_3, Sb_2O_3, H_2O_2 and KOH to obtain a slurry. The slurry has a molar composition of Ba:In:Sb:H_2O_2:KOH=2:1.05:1:0.5:10. Then, the mixture was subjected to strong stirring for 10 min. After that, the resulting mixture was transferred to a Teflon-lined stainless steel autoclave (ca. 20~30 cm^3 in capacity) and heated at 240~260 ℃ for 7 days with a filling factor ca. 80~85 vol.%. After cooling, the product was filtered out and washed with de-ionized water. Finally, the product was treated ultrasonically for several minutes with de-ionized water and dried at ambient temperature.

1.2 Characterization

XRD measurements were performed on a Rigaku D/max 2500 diffractomater in the 2θ range 10~120° with Cu $K\alpha$ radiation (λ=0.154 056 nm) at 40 kV and 120 mA, using a graphite monochromator. A scintillation counter filled with sodium metal was used as detector to count the diffraction intensity. The XRD data were obtained using a step length of 0.02° and count time of 8 s. The Rietveld method[8] was used to analyze the XRD data simultaneously with the General Structure Analysis System (GSAS) program[9]. The infrared spectrum was measured with a Bruker FT-IR Vector system using KBr pellets. After dissolving in hot hydrochloric acid of 6 mol·L^{-1}, metal ions of the product were determined using a Leeman Labs Plasma-Spec (I)AES. The product for electron microscopy was dispersed in methanol, and the electron diffraction (ED) study was carried out with an H-81001 V transition electron microscope under an acceleration voltage of 200 kV. The Sb binding energy was determined using a VG Scientific ESCA MAK-Ⅱ spectrometer with the pressure of 3×10^{-6} Pa and X-ray source of 1 253.6 eV, and calibrated in reference to C1*s*=285 eV.

The ^{121}Sb Mössbauer spectra were obtained in transmission geometry using a constant-acceleration spectrometer. The source was $Ca^{121m}SnO_3$ (~0.3 mCi) at room temperature. A proportional counter filled with xenon gas was used as detector to count the escape peak at about 8 keV produced by the 37.2 keV γ rays. The ^{121}Sb Mössbauer spectra were fitted by means of the least-squares method using the Mosswinn 3.0 software[10].

2 Results and discussion

2.1 Structure characterization

The XRD pattern of Ba_2InSbO_6 (Fig.1) shows a typical perovskite features, and some impurities are

identified as $KSbO_3$[11c], $BaSb_2O_6$[11b], $Ba_2In_2OH_{12}$[11c], Ba($Sb^{Ⅲ}$, $Sb^{Ⅴ}$)O_3[11d]. The elemental analyses indicate that the synthesized product has a metal composition of Ba∶Sb∶In≈2∶1∶1, which agrees with the double perovskite formula $A_2BB'O_6$.

The XRD pattern of Ba_2InSbO_6 was indexed with a cubic cell, and assigned to space group $Pm\bar{3}m$ with a= 0.416 782(13) nm. The data were first analyzed with a "whole pattern fitting" algorithm to determine accurately the profile shape function, background, and cell parameters. This prelimmary study provided good estimates of R_{wp} and χ^2 that could be reached during the structure refinement. The refinement converged to give an agreement factor R_{wp} =8.21% and χ^2 =1.57. The observed, calculated, and difference profiles are plotted in Fig.1. The structure parameters of Ba_2InSbO_6 are tabulated in Table 1.

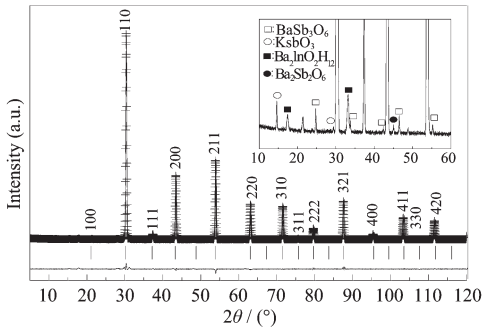

Crosses: observed; solid line: calculated; bottom solid line: difference; tick marks: Bragg reflections

Fig.1 Reitveld refinement profiles plot of XRD data of Ba_2InSbO_6 (The inset shows the detail features of impurities)

Table 1 Structure parameters of Ba_2InSbO_6 at room temperature[a]

Atom	Site	Position			Temperature parameter / ×100
Ba	1b	1/2	1/2	1/2	$U_{iso\ eq}$=1.060(29)
In / Sb	1a	0	0	0	$U_{iso\ eq}$=0.34(4)
O	3d	1/2	0	0	U_{11}=4.2(5)
					U_{12}=0.73(34)
					U_{13}=0.26(34

[a]Bond length: Ba-O: 0.294 709(7) nm, In/Sb-O: 0.208 391(7) nm.

A Goldschmidt tolerance factor (τ) of 1.0345 can be calculated for Ba_2InSbO_6. Perovskites with a tolerance factor equal to or greater than unity often exhibit no octahedral tilting[12], moreover, Ba^{2+} as A-cation is much bigger. Ba_2InSbO_6 with an aristotype cubic perovskite structure is possible. Large differences in size (greater than 0.02 nm) and / or oxidation state (greater than two) are two factors that favor cation ordering on the octahedral size[2]. The differences of charges and radii of B-cations in Ba_2SbInO_6 are two and 0.020 nm, respectively, existing at the place where random and rock salt sublattices meet[2]. Although, some literatures reported that In and Sb shows 1∶1 ordered in the B-cation rock-salt-type sublattice[2], however, both the reconstruction of reciprocal space from the selected area electron diffraction (SAED) patterns (Fig.2) and ^{121}Sb Mössbauer spectra (Fig.4) studies for the Ba_2InSbO_6 confirmed the disordering B-cations distribution and led to the space group $Pm\bar{3}m$, with a= a_P. As shown in Fig.2, the SAED images show no extra

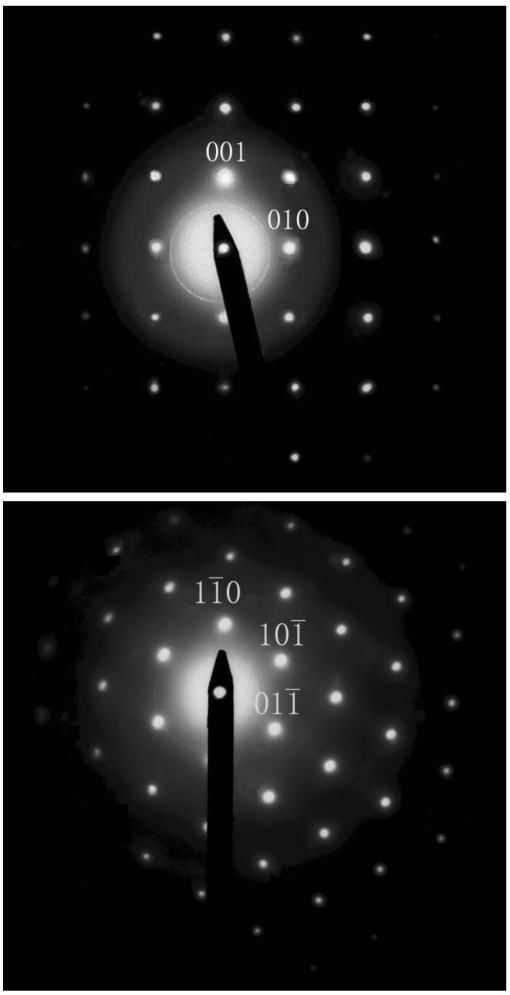

Fig.2 [100] and [111] SAED patterns index to an a_p-a_p-a_p cell and are in agreement with a $Pm\bar{3}m$ space group

weak spots, which attributes to the doubling of the cell parameters. As can be seen from the ^{121}Sb Mössbauer measurements, the line width of the broad peaks is evidently larger than the ideal value of 2.1 mm·s^{-1}. This indicates that the distribution of the In^{3+} and Sb^{V} ions at the center of the octahedron arrays is random.

The infrared spectrum (Fig.3) of Ba_2InSbO_6 shows two strong absorption bands around 660 cm^{-1} and ca. 400 cm^{-1}, and a weak band around ca. 850 cm^{-1}. In $A_2BB'O_6$-type perovskite, the highly charge B-cation octahedra, the SbO_6, act as independent groups, the vibration spectrum, therefore, arises from such SbO_6 octahedra. The two strong absorption bands around 660 and 400 cm^{-1} are assigned to the ν_3 and ν_4 modes of SbO_6 octahedra[7,13], respectively, and the weak absorption band at ca. 850 cm^{-1} is ascribed to ν_1 mode of SbO_6 octahedra. The ν_1 mode as a weak absorption band appears even if this mode usually is an infrared inactive vibration; then it becomes partially allowed due to the lowering of site symmetry[14]. This suggests that the B-cations are more than one type in Ba_2InSbO_6, and corresponding B-cations must be In^{3+} and Sb^{V} in the present work.

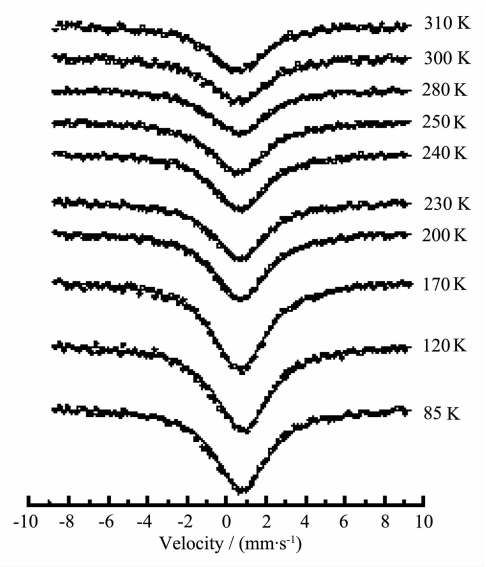

Fig.4　Temperature-dependence of the ^{121}Sb Mössbauer spectra of Ba_2InSbO_6

2.2　Mössbauer characterization and Antimony valence

^{121}Sb Mössbauer spectroscopy was applied for investigating the valence state of Sb in connection with powder XRD and XPS measurements. As shown in Fig.4, the ^{121}Sb Mössbauer spectra of Ba_2InSbO_6 at various temperatures are plotted. The Mössbauer parameters fitted by the least-squares method are tabulated in Table 2. The model of the powder static Hamiltonian mixed with quadrupole interaction and magnet interaction in Mosswinn was applied in the fitting of the spectra. The line width of the broad peaks is up to 3.07 mm·s^{-1} and evidently larger than the ideal value of 2.1 mm·s^{-1}. Since there is no amorphous component, this indicates that this result may cause asymmetric electronic environments around the antimony ions. Accordingly, it is certain that quadrupole splitting exists, although it has been suggested that the spectrum can be fitted with a single Lorentzian line[15].

Ba_2InSbO_6 only shows one symmetric absorption

Table 2　^{121}Sb Mössbauer spectral parameters for the Ba_2InSbO_6 at various temperatures

Temperature / K	IS[a] / (mm·s^{-1})	eQVzz / (mm·s^{-1})	η	H / T	Width / (mm·s^{-1})
85	0.42(2)	2.18 ± 0.34	0	1.14(7)	3.07(2)
120	0.43(2)	2.20 ± 0.34	0	1.14(7)	3.07(2)
170	0.37(2)	2.39 ± 0.34	0	1.06(7)	3.07(2)
200	0.35(2)	2.66 ± 0.34	0	0.89(7)	3.07(2)
230	0.32(2)	2.80 ± 0.34	0	0.39(7)	3.07(2)
240	0.29(2)	3.26 ± 0.34	0	0	3.07(2)
250	0.29(2)	3.46 ± 0.34	0	0	3.07(2)
280	0.26(2)	4.33 ± 0.34	0	0	3.07(2)
300	0.23(2)	4.38 ± 0.34	0	0	3.07(2)
310	0.22(2)	4.51 ± 0.34	0	0	3.07(2)

[a] Isomer shift is relative to $Ca^{121m}SnO_3$.

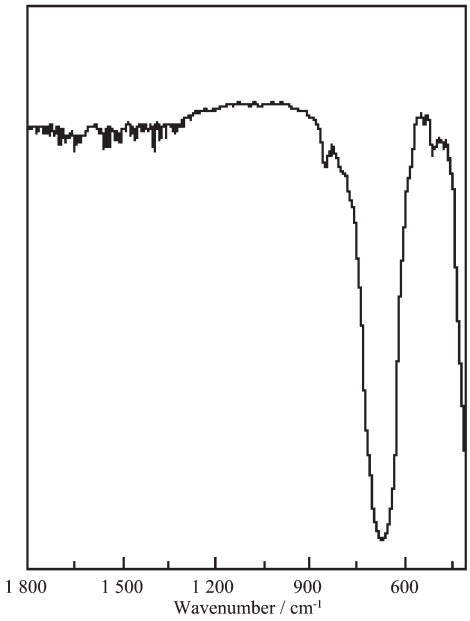

Fig.3 IR spectrum of Ba_2InSbO_6

peak, the values of all isomer shifts are in the range of 0.22~0.42 mm·s^{-1}. The ^{121}Sb Mössbauer method gives direct evidence that the antimony cations in Ba_2InSbO_6 are Sb^V rather than any other oxidation state or mixed valent. The high oxidation state of the Sb cations shows that Sb donates electrons to the conduction band instead of the occurrence of intervalence charge transfer. The electronic configuration is different from free-ion Sb^V where the 5*s* and 5*p* orbits are all empty. Some electrons occupy the valence-shell orbitals of the Sb cations since the energy band of Sb(5*s*) and O(2*p*) at the Fermi level is in the same range. According to literature [16], Ellis has calculated the valence-electron density as a function of the number of Sb 5*s* and 5*p* electrons by means of the tight-bonding method. Recently, Lippens[17] has related the values of the IS of antimonides with the valence-electron densities calculated by Ellis′s method. Based on these results, the electronic configuration $5s^m5p^n$ of Sb^V in Ba_2InSbO_6 was calculated to be corresponded to $m \approx 0.92$ and $n \approx 1.50$. The hybridization in Sb(5*s*, 5*p*) with the six neighboring O(2*p*) orbitals leads to covalent bonding character of the Sb-O bond.

As shown in Fig.5, the XPS spectrum of Sb further confirms the pentavalent Sb in Ba_2InSbO_6 oxide. The XPS spectrum gives the $3d_{3/2}$ and $3d_{5/2}$ of Sb^V binding

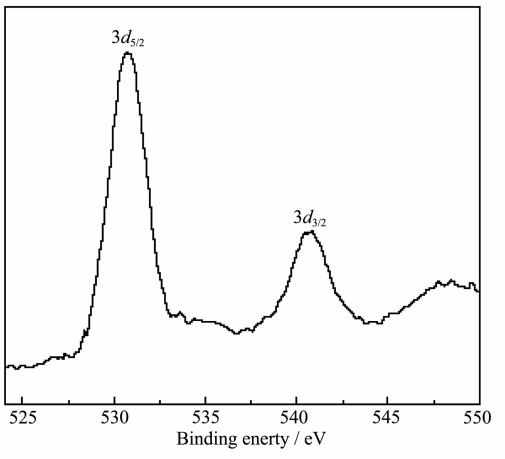

Fig.5 Sb^V $3d_{2/3}$ and $3d_{5/2}$ XPS spectrum of Ba_2InSbO_6

energies of 540.6 and 530.6 eV, respectively, and these peaks are typical profiles of Sb^V ion[18].

2.3 Formation of Ba_2InSbO_6

Suitable conditions for the synthesis were investigated by varying factors, such as, starting material of B-cations, alkalinity, reaction temperature and period. The Sb^V sources have significant influence on the synthesis of Ba_2InSbO_6. Dissoluble reactants, such as $SbCl_3$ and $SbCl_5$, used as the Sb^V sources, contribute to decrease in crystalline time, $Ba_2In_2OH_{12}$, $KSbO_3$, and $BaSb_2O_6$, however, often remain, as the impurities. When Sb_2O_3 and Sb_2O_5 are used as the Sb^V source, these antimony oxides can be used to the synthesis of Ba_2InSbO_6, but Sb_2O_3 is more efficient. Both of Sb_2O_3 and Sb_2O_5 possess a good solubility in alkali medium, whereas, in 1 to 16 mol·L^{-1} NaOH medium, Sb^{3+} exists as $Sb(OH)_4^-$ at concentration of 10^{-4} to 0.1 mol·L^{-1}, no polymeric species of Sb^{3+} appears in significant amounts at room temperature [19]. However, some polymeric species based on shared SbO_6 octahedra exist in $Sb(OH)_6^-$ solutions[19]. Sb_2O_3 as the Sb^V source may effectively control and reduce the nucleation of Sb^V in mixing process of reactants thus decreasing impurities formation. At reaction temperature, the lower concentration of Sb^V has limited the amount of polymeric species formed, meanwhile, the nucleation of Ba_2InSbO_6 becomes the preponderant one because perovskite-type product is favourable in terms of thermodynamic stability.

The solubility of $In(OH)_4^-$ is well established by the

solubilities of $In(OH)_3$ and In_2O_3 in basic solution. $In(OH)_4^-$ can form polynuclear species by condensation process, although $In(OH)_4^-$ is still a main form in basic medium[19]; thereby the influence of indium source is less than Sb^V source.

The crystallization process of Ba_2InSbO_6 may be probably attributed to dissolution-crystallization mechanism[20]. The crystallization process can be represented by the reaction as follows:

$$Sb(OH)_4^- + H_2O_2 \rightarrow Sb(OH)_6^- \quad (1)$$

$$In_2O_3 + 2OH^- + 3H_2O \rightarrow 2In(OH)_4^- \quad (2)$$

$$In(OH)_4^- + Sb(OH)_6^- + 2Ba^{2+} + 2OH^- \rightarrow Ba_2[InSbO(OH)_{12}] + H_2O \quad (3)$$

$$Ba_2[InSb(OH)_{12}] \rightarrow Ba_2InSbO_6 + 6H_2O \quad (4)$$

The $In(OH)_4^-$ ion has a lower tendency towards condensation but it may be incorporated with SbO_6 and easily enters into polyantimonate: antimonate behaves as polymerizable ligands, allowing the formation of mixed compounds, and indium adopts the same octahedral coordination as antimony in an alkaline medium. In addition, indium-antimony mixed hydroxyl-complex is energetically favored in comparsion with other hydroxyl-complex species for the synthesis of Ba_2InSbO_6.

The analysis of impurities in products further confirms the dissolution-crystallization mechanism. $Sb(OH)_6^-$ condenses to form antimonic acid $H_2Sb_2O_6$ with pyrochlore structure via dehydration in alkaline medium. In antimonic acid $H_2Sb_2O_6$, SbO_6 octahedra are connected by oxo bridges (corner sharing), and the solvated protons are distributed in the hexagonal channel of the structure[19]; however, at a given alkalinity, the solvated protons can be exchanged by alkali ions. Consequently, $Sb(OH)_6^-$ condenses to form $KSbO_3$ rather than $H_2Sb_2O_6$ in the present work, thereby $KSbO_3$ as an impurity is observed in as-synthesized products. Thus, pyrochlore-type oxide ($BaSb_2O_6$), formation is easy because Ba^{2+} and K^+ have similar crystalline radii (K^+:0.133 nm; Ba^{2+}:0.143 nm)[21]. Higher concentration of Sb^V conducts to the higher crystallization speed of Ba_2InSbO_6, nevertheless, the impurities grow rapidly too. This summary explains commendably the fact that Sb_2O_3 as Sb^V source is efficient in the present work.

3 Conclusions

A mild hydrothermal process allows coinstantane ous condensation between two kinds of B-cations to synthesize double perovskite oxide, where $A_2BB'O_6$-type Ba_2InSbO_6 particles with better crystallinity are obtained. The optimum temperature, alkalinity and reaction period are 240~260 ℃, 10 mol·L^{-1} KOH and 7 days, respectively.

^{121}Sb Mössbauer spectroscopy, XRD and XPS results indicate that the valence state of the Sb in this perovskite compound is only five, no mixed valence states is found. The change of the isomer shift with temperature is very small and can not be attributed to a change in valence state. The Sb-O bonds display some hybridized orbital characteristics and a small distortion along the z-axis is proposed.

References:

[1] (a)Crawford M K, Harlow R L, McCarron E M, et al. *Phys. Rev. B*, **1991**,**44**:7749~7756
(b)Thornton G, Jacobson A. *Acta Crystallogr. B*, **1978**,**34**:351~357
(c)Lufasoa M W, Macquarta R B, LeeY, et al. *J. Solid State Chem*. **2006**,**179**:917~922
(d)Fu W T, Ijdo D J W. *Ibid*, **2005**,**178**:2363~2367
(e)Fu W T, Ijdo D J W. *Solid State Commun*, **2005**,**134**:177~181
(f)Fu W T. *Ibid* **2000**,**116**:461~464
(g)Tauber A, Tidrow S C, Finnegan R D, et al. *Physica C*, **1996**, **256**:340~344

[2] Anderson M T, Greenwood K B, Talor G A, et al, *Prog. Solid State Chem*., **1993**,**22**:197~226

[3] Battle P D, Jones C W. *J. Solid State Chem*., **1978**,**78**:108~114

[4] (a)Byrappa K, Yoshimura M. *Handbook of Hydrothermal Technology-Technology for Crystal Growth and Materials Processing*, Noyes: William Andrew Publishing, **2001**.754
(b)Zheng W J, Peng W Q, Meng G Y. *Mater. Lett*., **2000**,**43**:19~22
(c)Zheng W J, Pang W Q. *Ibid*, **1997**,**33**:231~234
(d)Zheng W J, Pang W Q, Meng G Y. *J. Mater. Chem*., **1999**, **9**:2833~2836

[5] (a)Urban J J, Ouyang L, Jo M H, et al. *Nano Lett*., **2004**,**4**:1547~1550
(b)Lee B W, Cho S-B. *J. Eur. Ceramic Soc*., **2005**,**25**:2009~

2012
(c)Wang D, Yu Y B, Feng S H, et al. *Solid State Ionics*, **2002**, **151**:329~333
(e)Outzourhit A, Raghni M, Hafid M L, et al. *J. Alloys and Compounds*, **2002**,**340**:214~219
(f)Wang D, Yu R B, Feng S H, et al. *Mater. Res. Bull*, **2001**, **36**:239~244
(g)Zheng W J, Pang W Q, Meng G Y, Solid S tate Ionic, **1998**, **108**:37~41
(h)Zheng W J, Liu C, Yue Y, et al. *Mater. Lett.*, **1997**,**30**:93~96
[6] (a)Spooren J, Walton R I. *J. Solid State Chem.*, **2005**,**178**:1683~1691
(b)Liu J B, Wang H, Zhu M K, et al. *Mater. Res. Bull*, **2003**, **38**:817~822
(c)Zhu D L, Zhu H, Zhang Y H. *J. Crystal Growth*, **2003**,**249**:172~175
(d)Zhang T, Jin C G, Qian T, et al. *J. Mater. Chem.*, **2004**,**14**:2787~2789
(e)Spooren J, Walton R I, Millange F. *Ibid*, **2005**,**15**:1542~1551
(f)Spooren J, Rumplecker A, Millange F, et al. *Chem. Mater.*, **2003**,**15**(7):1401~1403
(g)Xu G, Ren Z H, Du P Y, et al. *Adv. Mater.*, **2005**,**17**(7):908~910
(h)Zhu D L, Zhu H, Zhang Y H. *Appl. Phys. Lett.*, **2002**,**80**(9):1634~1636
(i)Chen X L, Fan H Q, Ke S M. *Ibid*, **2006**,**88**:2901~2904
(j)Suyal G, Colla E, Gysel R, et al. *Nano Lett.*, **2004**,**4**(7):1339~1342
[7] (a)Wu L Y, Mei X Y, Zheng W J. *Mater. Letter*, **2006**,**60**:2326~2230
(b)ZHENG Wen-Jun(郑文君), HUANG Hong-Bo(黄红波), WU Li-Yan(武丽艳), et al. *Chemical J. Chinese Univ.* (*Gaodeng Xuexiao Huaxue Xuebao*) **2004**,**25**:2199~2203
(c)Huang H B, Zheng W J, Dai Y D, et al. *Physica B-Condensed Mater*, **2003**,**328**:271~2751
(d)Zheng W J, Pang W Q, Meng G Y, et al. *Mater. Letter*, **1998**, **37**:276~280
[8] Rietveld H M. *J. Appl. Crystallogr*, **1969**,**2**:65~76
[9] Larson A C, Von Dreele R B. *GSAS-General Structure Analysis System; Los Alamos National Laboratory Report No. LAUR* 86-748, Los Alamos: Los Alamos National Laboratory, NM, **2000**
[10]Klencsar Z. *Nucl. Instrum. Methods B*, **1997**,**129**:527~534
[11](a)PDF: 46-1494
(b)PDF: 49-0165
(c)PDF: 30-129
(d)ZHENG Wen-Jun(郑文君), PANG Wen-Qin(庞文琴), *J. Inorg. Mater.*(*Wuji Cailiao Xuebao*), **2000**,**15**:275~279
[12]Lufaso M W, Woodward P M. *Acta Cryst. B*, **2004**,**60**:10~20
[13]Lawat A E, Baran E J. *Vibrational Spectroscopy*, **2003**,**32**:167~174
[14] (a)Nyguist R N, Kagel R O. *Infrared Spectra of Inorganic Compounds*. New York: Academic Press, **1971**.
(b)Nakamoto K. *Infrared and Raman Spectra of Inorganic and Coordination Compounds*. New York: Wiley, **1986.**
[15]Eibschtz M, Reiff W M, Cava R J, et al. *Appl. Phys. Lett.* **1991**,**58**:2848~2850
[16]Ruby S L, Shenoy G K. *Mössbauer Isomer Shift*. Amsterdam: NorthHolland, **1978**.623
[17]Lippens P E. *Solid. State Commun*. **2000**,**113**:339~403
[18]*Standard Esca Spectra of the Elements and Line Energy Information*, USA:ΦCo. **1990.**
[19](a)Jolivet J P, Henry M, Livage J, et al. *Metal Oxide Chemistry and Synthesis*. Chichester: John Wiley & Sons LTD, **1994.**
(b)Baes C F, Jr Mesmer R E. *The Hydrolysis of Cations*, New York: John Wiley & Sons, Inc., **1976**.
[20]Hou B, Li Z J, Xu Y, et al. *Chemistry Letters.*, **2005**,**34**:1040~1041
[21]Paoling L. *The Nature of the Chemical Bond*, Cornell: Cornell University Press, **1960**.504